Systematics of *Kα* X-ray Satellite Peak Widths

V. Horvat, R.L. Watson, and Y. Peng

Spectra of $K\alpha$ x rays emitted from a variety of solid targets (atomic number Z_2 = 17-32) under bombardment by fast heavy ions (atomic number Z_1 = 6-93) at 2.5-25 MeV/amu were measured in high resolution using a curved crystal spectrometer. The spectra were analyzed in order to examine the systematics of $K\alpha$ x-ray satellite structure [1]. In this report the focus is on the Gaussian widths of the satellite peaks.

Structure of the measured spectra was described in terms of a background function (a constant in most cases) and 18 peaks having Voigt profiles. The peaks represented the contributions from $K\alpha_1$ and $K\alpha_2$ diagram transitions as well as those from $K\alpha_1 L^i$ and $K\alpha_2 L^i$ satellite transitions (i = 0, 1, 2, 3, 4, 5, 6, 7). Here index i represents the number of spectator L vacancies at the time of the $K\alpha$ x-ray transition, while the number of spectator outer-shell vacancies (in the M shell or above) is unspecified.

A Voigt function is a convolution of a Gaussian function and a Lorentzian function. For the most part, the width of the Lorentzian component represents the natural transition width, which was fixed based on the literature values of level widths [2]. For a single diagram peak, the Gaussian component width of the Voigt function represents the resolution of the spectrometer. This parameter was varied in order to obtain the best fit to the diagram peaks in each measured spectrum.

Gaussian component widths of the peaks representing $K\alpha_1 L^i$ or $K\alpha_2 L^i$ satellite transitions were in most cases fitted independently from each other and from all other parameters of the fit, because each one of them is determined primarily by the distribution of a large number of unresolved transitions having a range of transition energies that contribute to the given satellite peak. The spread of transition energies is due to the coupling of electronic angular momenta before and after the x-ray emission, as well as due to the probability distribution of outer-shell vacancy configurations. For the satellite peaks that were not resolved from other peaks and represented a relatively small fraction of the satellite peak distribution, Gaussian widths could not be fitted independently. Instead, their values were estimated and held constant. However, those values were *not* included in the analysis described below.

Independently determined Gaussian component widths of the satellite peaks were grouped according to their associated numbers of spectator L vacancies (i) and the target atomic number (Z_2), regardless of the projectile atomic number and projectile energy. The data in each group were then replaced by their average value $\sigma_s(i, Z_2)$. A similar procedure was applied to the Gaussian widths of the diagram peaks. They were sorted in groups based on Z_2 and then the data in each group were replaced by their average value $\sigma_d(Z_2)$. The differences $\Delta\sigma(i, Z_2) = \sigma_s(i, Z_2) - \sigma_d(Z_2)$ are shown in Fig. 1 on the top left and top right, as a function of i and Z_2, respectively. The curves in the graphs represent the results of unconstrained linear regression applied to each individual set of data with the given values of i or Z_2. Based on the trends observed in the two graphs, it was found that $\Delta\sigma(i, Z_2)$ can be approximated by

$$\Delta\sigma(i, Z_2) = a_1\, i\, (a_2 - i)\, (Z_2 - a_3)\ , \qquad (1)$$

where a_1, a_2, and a_3, are constants. Their best-fit values were found to be

$$a_1 = 0.0246 \pm 0.0018 \qquad a_2 = 9.86 \pm 0.23 \qquad a_3 = 10.40 \pm 0.74\ . \qquad (2)$$

Figure 1 on the bottom left and bottom right illustrates how well the data points are represented by eq.(1). On the bottom left $\Delta\sigma(i, Z_2) / (Z_2 - a_3)$ is plotted as a function of i, while on the bottom right $\Delta\sigma(i, Z_2) / [i\,(a_2 - i)]$ is plotted as a function of Z_2. The data points in these graphs represent the average values of all the derived data points at the given value of the abscissa, while the error bars represent sample standard deviations.

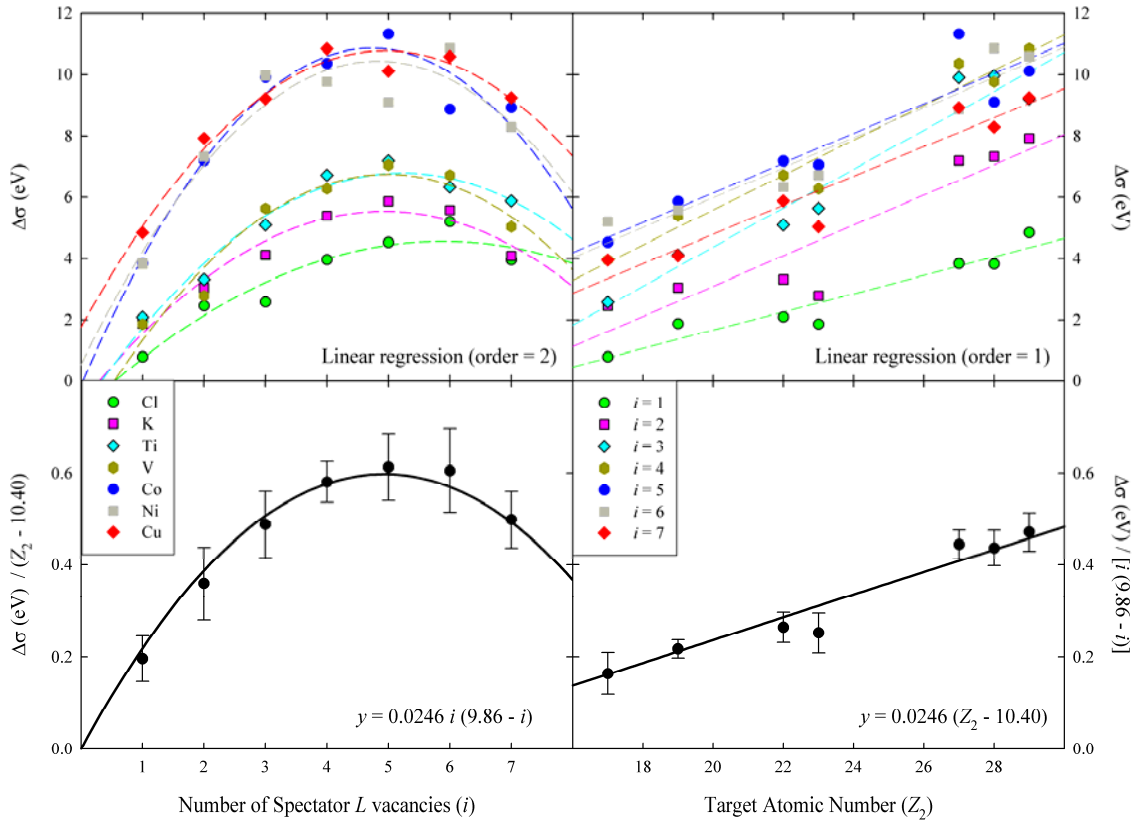

Figure 1. Systematics of the satellite peak widths.

[1] V. Horvat *et al.*, *Progress in Research*, Cyclotron Institute, Texas A&M University (2004-2005), p. IV-9.

[2] J. L. Campbell and T. Papp, At. Data Nucl. Data Tables **77**, 1 (2001).